

LCLS-II INJECTOR OPERATIONAL CHALLENGES AND DEVELOPMENTS*

F. Zhou[†], A. Brachmann, D. Cesar, W. Colocho, Y. Ding, D. Dowell, G. Just, A. Osman, N. Sudar, T. Vecchione, Z. Zhang, and C. Zimmer
SLAC National Accelerator Laboratory, Menlo Park, United States

Abstract

The Linac Coherent Light Source II (LCLS-II) has been in user operations since 2023 and has successfully ramped up the beam repetition rate to 93 kHz. The LCLS-II photoinjector has demonstrated the ability to deliver a high-brightness, low-emittance electron beam at high repetition rates, meeting key performance targets. However, several operational challenges have emerged during commissioning and user operation. These include substantial gun dark current, degradation of cathode quantum efficiency (QE) uniformity, unexpected electron beam breakup, significant emittance growth through the laser heater chicane, the presence of beam halos, and cathode QE dependence on e-beam rate. This paper provides an overview of these challenges and highlights recent efforts to address these outstanding issues and discusses plans for further improvement of the performance.

INTRODUCTION

Continuous-wave (CW) free-electron laser (FEL) facilities such as LCLS-II impose stringent requirements on the photoinjector to deliver high-brightness, low-emittance, and reliable electron beams. The LCLS-II 1 MeV electron source was successfully commissioned between 2018 and 2020, following the resolution of several significant technical challenges [1]. In 2022, the full-scale >70 MeV injector was commissioned, and its beam performance was then characterized and optimized. Figure 1 presents a schematic layout of the complete injector.

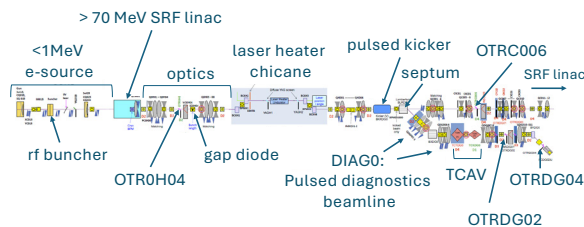


Figure 1: Schematic of the LCLS-II injector layout.

The injector consists of the 1 MeV electron source, a >70 MeV standard cryomodule (CM01), a laser heater chicane, and multiple diagnostic stations. These include the first emittance station (OTR0H04) and a gap diode for relative bunch length measurements, both located before the laser heater chicane; a second emittance station (OTRC006) located downstream of the chicane; and a dedicated off-axis diagnostics station equipped with a

transverse deflecting cavity (TCAV) for absolute bunch length measurement, along with an additional emittance measurement station.

Since the start of FEL user operations in 2023, a variety of operational challenges have been encountered in the injector system. This paper discusses the key issues and the corresponding efforts toward their resolutions, including:

- Improvement of gun vacuum 10-fold after processing major low energy multipacting barriers.
- Mitigation of large gun dark current, significantly reducing dark current loss downstream in high energy area.
- Observation of the formation of QE crater/bump on the photocathode within weeks of operation, resulting in spatial and charge instability in the beam and emittance dilution, and QE dependence of the beam rate.
- Correction of stray magnetic fields in the laser heater chicane, mitigating emittance growth.
- Observation of beam halos and mitigation with new bunching scheme.
- Maintaining low beam emittance.
- Observation of harmonic laser energy modulation through laser heater chicane.

PERFORMANCE AND OPERATIONAL CHALLENGES

The following sub-sections present an overview of major operational challenges and the systematic efforts undertaken to diagnose and resolve them.

CW Gun Operational Improvements

The gun vacuum gradually degraded over time, increasing from 8×10^{-10} Torr in 2023 to 2×10^{-9} Torr by December 2024. In October 2024, a small step-like increase in vacuum pressure was observed; however, the source of this change remained unidentified until December 2024, when a vacuum leak was discovered on one of two RF windows. Following the identification of the leak, the faulty window was replaced, and the entire gun assembly was baked at $150\text{--}170^\circ\text{C}$. During following RF power processing of the gun, we processed through all major multipacting barriers this time rather than jumping over these barriers for rapidly increasing the RF power to nominal in the past, resulting in a significant improvement in vacuum conditions. The base pressure with CW RF on was improved by 10-fold. The gun vacuum has remained stable at 2.4×10^{-10} Torr over the five months of operation following the RF processing.

*Work supported by US DOE Contract
[†]zhoufeng@slac.stanford.edu

Gun Dark Current Mitigations

The CW normal-conducting RF gun generates 2-3 μA of dark current, primarily originating from localized emission sites near the rim of the 10 mm-diameter cathode plug. This dark current presents a significant risk to the permanent magnets in the undulator sections due to potential radiation-induced damage. To mitigate this risk, a circular collimator was firstly installed to intercept the dark current at low energies (<1 MeV), thereby reducing radiation production. The collimator, with a 20 mm aperture, effectively blocks approximately 90% of the dark current, resulting in a manageable power loss of only 1–2 W and negligible impact on the photo-injected beam. However, the remaining $\sim 10\%$ of dark current is accelerated through the cryomodules, causing beam losses at various downstream locations. These losses have led to frequent damage to camera systems and laser energy meter electronics, the formation of localized hot spots, and beam loss events.

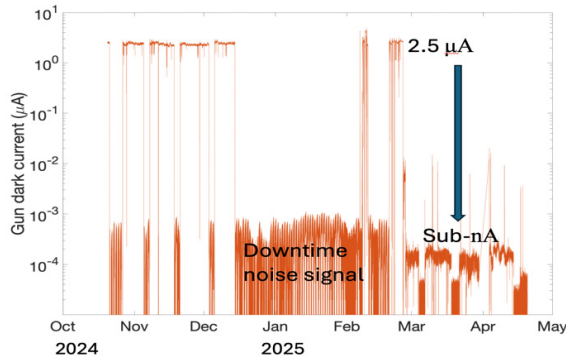


Figure 2: Log of the gun dark current vs. months with standard flat cathode, and over-inserted cathode beginning Feb 25, 2025.

In 2024, a 1-mm over-inserted cathode was developed [2], to reduce the dark current propagating downstream through the beamline. This design lowers the electric field gradient at the nose of the cavity, which has been identified as the primary source of gun dark current. Additionally, the increased defocusing effect helps steer the dark current away from the cathode axis, significantly reducing the dark current transported through the first cryomodule CM01 and downstream. In addition, the modified geometry enhances the electric field gradient at the cathode surface, which improves beam emittance based on simulation. The over-inserted cathode was deployed at the LCLS-II injector on February 25, 2025, leading to a dark current reduction of more than 1000-fold, as shown in Fig. 2. This dramatic improvement has substantially enhanced machine availability and beam quality.

Formation of Cathode's QE Crater and Bump

Cs_2Te cathodes grown at SLAC have been used in LCLS-II operations. It has been observed that all cathodes exhibit a similar evolution of QE: an initial QE crater is formed after few days of operation, followed by the development of a QE bump over weeks. Figure 3 shows the QE bump for three illumination laser spots. Beam operation

begins at laser location 1. After a few days, a QE crater is first observed (not shown in the image). Over time, the QE gradually increases, forming a localized bump over weeks (left). Because this QE bump degrades beam quality and stability, and causes QE dependence of the beam rate, the laser is then moved to a new location, spot 2 (middle). At spot 2, the QE initially decreases after a few days of operation (not shown in the image), then gradually increases, and eventually a QE bump is formed that was observed at spot 1. Meanwhile, the QE at spot 1 diminishes when it is no longer illuminated with the laser. When the laser is moved to spot 3, the same sequence of behavior is observed (right), indicating a reproducible pattern across different locations on the cathode.

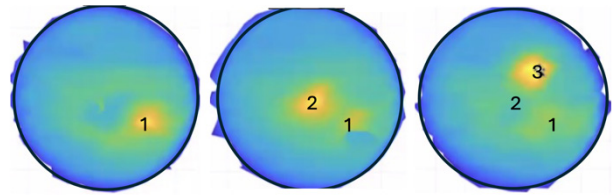


Figure 3: Formation of QE bumps and diminishment.

We believe that the QE crater/bump behavior is related to cathode parameters, such as base material, Cs thickness and temperature, and laser-induced desorption and diffusion. Optimization of the cathode parameters and related studies are currently underway. The goal is to mitigate the QE crater/bump formation.

Correction of Stray Field for Emittance Preservation

Below half-micron emittance is achieved at the 1st injector emittance station. However, emittance growth, by a factor of 2 to 3, was observed at the 2nd injector emittance station, located downstream of the laser heater chicane. Figure 4 shows measured emittances at the first (top left) and second (top right) emittance stations, where a typical doubling of emittance is evident after the beam passes through the chicane. Also, achieving consistent beam optics matching at the 2nd station was challenging.

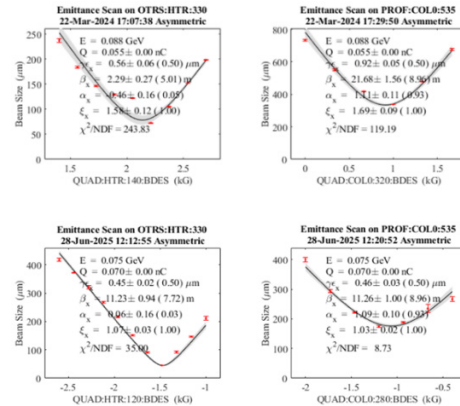


Figure 4: Emittance before (top) and after (bottom) correction of the stray field at the 1st (left) and 2nd (right) emittance stations.

Investigations revealed that low-carbon steel plates were used to support lead shielding near the 2nd bend of the laser heater chicane. Modeling indicated that these steel supports introduced magnetic field perturbations of 1–3% for the 2nd dipole, which may distort the beam optics and contribute to emittance degradation. To correct this, the low-carbon steel was replaced with non-magnetic stainless steel for the shielding support structures. Following this modification, emittance through the chicane is well-preserved. Figure 4 shows the comparisons of the emittance measurements taken before (top) and after (bottom) the replacement.

Beam Breakup and Mitigation

A split or donut-shaped beam profile was frequently observed on both injector screens, as shown in Fig. 5 (left) as an example. This beam deformation had a direct and detrimental impact on FEL performance. Systematic modeling identified space charge effects due to the small size of the drive laser spot on the cathode—as the primary cause of the observed beam distortion. To address this issue, the laser size diameter was increased from 0.65 mm to 0.8 mm. With proper solenoid field, the split beam structure was reasonably eliminated, as shown in Fig. 5 (right) without compromising beam emittance.

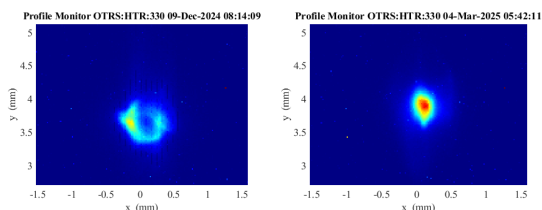


Figure 5: e-beam profile at the 70 MeV with smaller (left) and relatively larger (right) laser sizes.

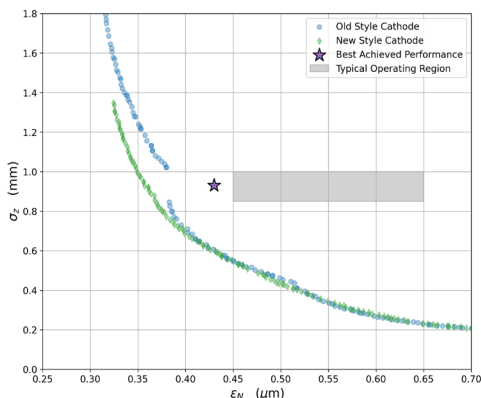


Figure 6: Best injector emittance as well as routine emittance during operation at 75 pC.

LCLS-II Injector Emittance

LCLS-II injector emittance is measured at the screen OTR0H04 downstream of CM01. Figure 6 shows the measured best injector beam emittance as well as the routine emittance during operation at 75 pC charge and desired 1 mm bunch length, in comparison to the simulations. The best measured emittance is close to the simulation, but it

cannot be routinely maintained due to inconsistent laser spatial profile and non-uniform electron emission from the cathodes as mentioned in the above sub-section. In 2026, a few upgrades are being pursued:

- The laser system is being upgraded to improve laser stabilities (pointing and energy) and laser profile.
- The cathode growing parameters (base material, Cs thickness) are being optimized for mitigation of the QE crate/bump.

Beam Halos

Beam halo has been observed on the injector screens. Further simulations [3] reveals that 1) the RF buncher induces an energy-radius correlation, 2) velocity bunching through the buncher transforms this correlation into hollow density structures, and 3) differential over-focusing of these structures by downstream focusing forms the beam halos. To mitigate the effect, we implemented a two-stage velocity bunching: one part from the RF buncher and another part from the second cavity of CM01. With this approach the space charge effect is mitigated with less bunching from the buncher at low energy and additional bunching from the 2nd cavity of CM01 at relatively higher energy. Experimental results [3] confirm that beam halo is mitigated with the new bunching scheme compared to the bunching from buncher only.

Third Harmonic Laser Heater Modulation

The injector beam energy is lower than the design as the energy gain from CM01 is limited [4] due to its unexpected field emission. We decide to first commission the laser heater undulator at the 3rd harmonic resonance energy, ~75 MeV with 30 mm of undulator gap. To enhance the modulation amplitude, the laser heater pulse length is reduced from the nominal 18 ps to 2 ps. Since the electron bunch has a full width of about 15 ps, significantly longer than the laser pulse, this results in a localized sliced energy modulation within the bunch, as shown in Fig. 7.

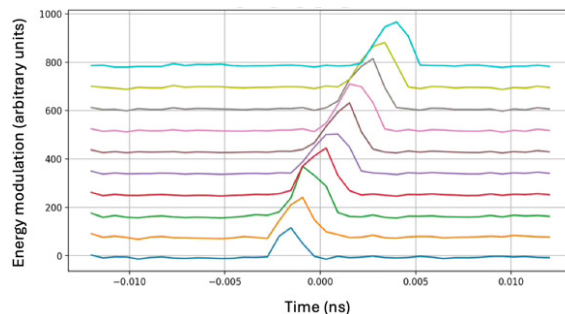


Figure 7: Localized sliced energy modulation within the bunch.

REFERENCES

- [1] F. Zhou *et al.*, “Commissioning of the SLAC Linac Coherent Light Source II electron source”, *Phys. Rev. Accel. Beams*, vol. 24, p. 073073401, 2021. doi:10.1103/PhysRevAccelBeams.24.073401
- [2] T. Luo and D. Dowell, “Recent new cathode development for LCLS-II photoinjector”, *AD forum*, SLAC, July 18, 2025.

- [3] Z. Zhang *et al.*, “Beam halo formation via longitudinal-transverse coupling in CW photoinjectors”, in preparation for publication, 2026.
- [4] L. Alsberg *et al.*, “LCLS-SC operation status and the LCLS-II-HE upgrade”, to appear in SRF2025, Tokyo, Japan, 2025.